Accepted Manuscript

Investigation into Mode II interlaminar fracture toughness characteristics of flax/basalt reinforced vinyl ester hybrid composites

F.A. Almansour, H.N. Dhakal, Z.Y. Zhang

PII: S0266-3538(17)32470-3

DOI: 10.1016/j.compscitech.2017.11.016

Reference: CSTE 6971

To appear in: *Composites Science and Technology*

Received Date: 29 September 2017

Revised Date: 15 November 2017

Accepted Date: 16 November 2017

Please cite this article as: Almansour FA, Dhakal HN, Zhang ZY, Investigation into Mode II interlaminar fracture toughness characteristics of flax/basalt reinforced vinyl ester hybrid composites, *Composites Science and Technology* (2017), doi: 10.1016/j.compscitech.2017.11.016.

Investigation into Mode II interlaminar fracture toughness characteristics of flax/basalt reinforced vinyl ester hybrid composites

F.A. Almansour *, H.N. Dhakal and Z.Y. Zhang
Advanced Polymers and Composites (APC) Research Group, School of Engineering, University of Portsmouth, Portsmouth, Hampshire, PO1 3DJ, United Kingdom.

Abstract

In this work, the influence of water absorption of flax and flax/basalt hybrid laminates is presented with the aim to investigating the Mode II interlaminar fracture toughness. Four types of composite laminates namely, neat vinyl ester (neat VE), flax fibre reinforced vinyl ester (FVE), flax fibre hybridised basalt unstitched (FBVEu) and flax hybridised basalt stitched (FBVEs), were fabricated by vacuum assisted resin infusion technique. Three-point-end-notched flexure (3ENF) tests were performed to evaluate the critical Mode II strain energy release rate (G_{IIC}) and the crack length (R-curve) at dry and wet conditions, by using two data reduction methods. The morphology of delamination and the fracture shear failure of composite laminates were evaluated using scanning electron microscopy (SEM) and X-ray micro computed tomography (µCT). The results obtained that the fracture energy of FBVEu composites, $G_{IIC\ init}$. and $G_{IIC\ prop.}$ were increased by 58% and 21%, respectively compared to that of FVE dry specimens. Moisture absorption phenomenon caused increasing in the ductility of matrix that improved the resistance to crack initiation. However, this was inverted to a reduction in the fibre/matrix interfacial strength of FBVEu wet composites and a deterioration in the delamination resistance to crack propagation. The critical strain energy release rate of neat VE increased from 157.84 J/m^2 to 239.85 J/m^2 with reinforcement of flax fibre composites. The experimental results confirmed that basalt fibre hybridisation enhanced the durability and water repellence behaviour of natural fibre reinforced composites.

Keywords: A. Flax fibres; A. Hybrid composites; B. Fracture toughness; B. Delamination.

* Corresponding author. Tel.: +44 (0) 23 9284 2586.
E-mail address: fahad.almansour@port.ac.uk (F.A. Almansour).

1. Introduction

In the last two decades, natural plant fibres as reinforcements in polymer composites have been extensively used towards achieving sustainable green materials. The key factor that drives in focusing on the use of natural plant fibre-reinforced polymer (FRP) composites over synthetic FRPs is ecological advantages: availability, renewable resources and biodegradability, which reduce large amounts of embodied energy [1]. Among the different types of natural fibres, bast fibres (flax, hemp, jute and ramie) derived from plants are most commonly used in different applications such as automotive, marine and construction, because of their attractive properties in terms of weight (low density) and performance (high specific strength and modulus) [2]. In recent years, there has been resurgence for using these fibres as reinforcement in composite materials. This renewed interest is attributed to increasing prices of non-renewable oil products and new strict environmental regulations [3].

Despite aforementioned advantages, some of the main challenges for the use of natural plant fibres are susceptibility to moisture absorption that leads to poor adhesion between fibre and matrix interface due to the presence of hydroxyl and polar groups in composites. The diffusion of water in the composite materials can cause swelling and plasticisation that could effect the mechanical and thermal properties [4]. Dhakal et al. [5] studied the effect of water absorption on the mechanical properties of flax and jute reinforced bioresin composites. The results showed that the percentage of moisture uptake for jute composites were higher than that of flax samples. The flexural strength and modulus for both samples were decreased after immersed in distilled water at 25 °C for 961 hours. The flax wet samples reduced 40% of its strength and 69% of modulus, whilst the jute wet composites lost 60% of its strength and 80% of modulus. In addition, Chow et al. [6] found that the tensile strength and modulus of sisal reinforced polypropylene composites decreased after water immersion at elevated temperature of 90 °C for different durations. The decreased properties can be attributed to the plasticisation of sisal fibre composites interface and swelling of fibres.

Natural FRP composites are still limited in non-structural applications due to their higher moisture absorption, lower strength and stiffness properties [7]. To tackle these issues, a hybridisation of natural cellulosic fibres with mineral fibres which have superior ageing resistance and thermal resistance were investigated to improve the mechanical properties. At the present time, there is a significant interest for using basalt fibres as hybridising material into natural FRP composites due to their excellent properties such as mechanical, chemical, thermal and acoustic insulation [8–10]. Fiore et al. [8] investigated the effects of basalt fibre hybridisation as a double external layers on the impact and flexural properties of flax reinforced composites under different environmental conditions. They found that the impact, flexural strength and modulus of flax/basalt hybridised composites were higher than flax without hybridisation by 28%, 71% and 49%, respectively. Similar work carried out recently by Fiore et al. [9] on jute-basalt fibre reinforced hybrid structures highlighted that all composite laminates performed lower in their mechanical properties with increasing ageing time but the sandwich structure of basalt hybrid performed best in terms of their mechanical performance compared to other generic composites. The properties enhancement realised can be related to positive attributes of basalt fibre. Basalt fibres are obtained from mineral through melting rocks, thus non-hazardous/toxic which can be considered as environmentally friendly material compared to glass fibres [11,12]. Therefore, basalt hybridisation into natural fibres can serve as an effective means to enhance the mechanical properties and moisture resistance of composites by promoting improved fibre/matrix interface. From these benefits, the capability of the basalt fibres to be used as a hybridisation for a structural reinforcement material is extremely expected [13].

Based on reviewed literature, it is evident that most of the studies have been carried out investigating the properties of natural FRPs exposed to the durability of moisture absorption [5,6,12,14,15]. Majority of these studies focus on the mechanical properties, very few works on fracture toughness have been carried out on natural FRP composites [16–20]. Moreover, there are hardly any research works that comprehensively studied the effect of water absorption on the interlaminar fracture behaviour of natural FRPs in terms of understanding their properties of fracture energy and crack length [21]. The delamination and crack propagation of natural FRP composites depends on several factors such as fibre volume fraction [17,19], fibre/matrix interface [16,22], fibre orientation angle [17,23] and mechanical properties of the materials [19,24]. Study by Liu and Hughes [17] revealed that the fracture toughness is strongly dependent on the stacking sequence and weave configuration of the textiles when composites tested under different weft or warp directions. Hughes et al. [25] investigated the fracture toughness of bast fibres of hemp and jute reinforced polyester composites as well as unsaturated polyester neat in comparison to chopped strand mat (CSM) glass fibre laminates. The results showed that the critical strain energy release rate G_C, was significantly higher for CSM laminates than hemp, jute and unreinforced polymer composites of 10.21, 1.84, 0.97 and 0.10 kJ m^{-2}, respectively at 20% fibre volume fraction. Almansour et al. [26] highlighted that non-woven flax/basalt hybridised laminates improved the fracture toughness compared to non-woven flax composites without hybridisation using 3ENF testing. It was reported that the critical strain energy release rate G_{IIC}, and stress intensity factor K_{IIC} were increased for flax/basalt laminates by 12% and 33%, respectively compared to flax composites without hybridisation. Wong et al. [19] characterised short bamboo fibre reinforced polyester composites and neat polyester using compact tension (CT) specimens with different fibre volume fractions from 0 to 60 vol.% at 4, 7 and 10 mm fibre lengths, respectively. The results showed that the highest fracture toughness of hybrid composites was achieved with improvement of 340% compared to neat polyester, whereas the fracture toughness decreased incrementally of 10, 7 and 4 mm at 50, 40 and 10 vol.% with critical stress intensity factors, K_{IC}, of 1.73, 1.62 and 1.50 MPa $m^{1/2}$, respectively.

In general, delamination corresponds to stable and unstable crack between the plies in composite applications ascribed to inherent defects from the materials or through process fabrication and also damage incurred during the service life when composite undergoes to different loading and environmental conditions [27]. Therefore, there are some methods to reduce the interplay delamination by using toughened matrix, woven fabrics, through-thickness stitching and interleaving [28]. Previous studies have investigated the effect of stitching on the Mode II interlaminar fracture toughness of FRPs [29–31], but natural fibres composites still not yet reported. It was reported that the addition of stitching improved the mode II delamination resistance up to four times and observed stable crack propagation of FRPs, which depended on the parameters of stitch density, thread type and dimeter [31]. Ravandi et al. [32] have reported the effect of through-thickness natural fibre stitches on the low-velocity impact of woven flax reinforced epoxy composite laminates. Stitching of flax yarn led to decrease the intralaminar fracture toughness of woven flax composites about 16%, whereas the cotton yarn stitching was reduced by only 5 %.

This paper aims at investigating the Mode II interlaminar fracture toughness of woven flax and flax/basalt reinforced vinyl ester composites. In addition, the influence of water absorption on the fracture toughness behaviour of composite laminates was evaluated. Three-point-end-notched flexure (3ENF) tests were carried out to measure the crack length and the critical strain energy release rate, G_{IIC} (initiation and propagation). The shear fracture surfaces of woven flax and flax/basalt hybrid and stitch composites were analysed to understand the failure mechanisms of delamination and crack growth resistance.

2. Materials and experimental procedure

2.1 Materials

Woven flax and basalt fibres were used as the reinforcements of fibre orientation $[\pm45]_{3s}$ biaxial stitched non-crimp fabrics of 600 g/m^2 in aerial weight, supplied by Net Composites Ltd and Basaltex NV (Belgium), respectively. The matrix used was vinyl ester and obtained from Scott-Bader, named Crystic VE676-03. Crystic accelerator 'G' was added with the resin to accelerate gel time at 2% by weight and mixed along with Triganox 239 at 2% by weight as the catalyst. The Teflon layer of PTFE in 20 μm was used to simulate a crack in the reinforced composite panels.

2.2 Fabrication of composite laminates and test specimens

Composite laminates of flax fibre reinforced vinyl ester (FVE), flax fibre hybridised basalt reinforced vinyl ester, unstitched (FBVEu) and flax fibre hybridised basalt reinforced vinyl ester, stitched (FBVEs) were fabricated using vacuum assisted resin transfer moulding (VARTM) technique. In FVE composite laminates, six layers of woven flax were used with fibre weight content of 100%. The hybridised composites of FBVE were used by replacing two external layers of woven flax by two layers of woven basalt, with fibre weight ratio of flax/basalt, (70:30). Stitched panels were included three single rows at 2 mm intervals after the crack tip of 5 mm by using sewing machine. Stitching was done prior to infusion to hold all layers of the dry fabric together. Vacuum infusion process have been explained in details in our previous work [21]. The void content was 4.5% and was calculated according to ASTM D2734-94. Test specimens were cut from the panels by using water jet machine. After that instantly dried the specimens at 50 °C for 24 hours to remove any moisture absorbed.

2.3 Moisture absorption tests

Four specimens of each composite laminate type were immersed in distilled water after desiccating process at room temperature 23 °C. After 24 hours intervals, specimens were removed from the water and their surface moisture was dried using tissue paper to measure the weight immediately. This step was repeated for 42 days (1008 hours) until it reached to the saturation state. The effect of moisture absorption on Mode II interlaminar fracture toughness of neat VE, FVE, FBVEu and FBVEs were investigated in accordance with BS EN ISO: 1999 to calculate the moisture uptake percentage and the diffusion coefficient of different composites.

Moisture absorption was calculated by measuring their weight gain. The moisture uptake in percentage $M_{(\%)}$ was determined as follows:

$$M_{(\%)} = \frac{W_t - W_0}{W_0} \times 100 \qquad [1]$$

Where, W_0 is the initial weight of the sample at dry condition; W_t is the weight of water immersed specimens at a given time.

The diffusion coefficient (D) was determined using the following equation:

$$D = \frac{d^2}{\pi^2 \times t_{70}} \qquad [2]$$

Where, d is sample thickness (mm) and t_{70} is time taken to reach 70% of saturation (s).

The diffusion coefficient (D) is defined as the slope of the normalised mass uptake against square root of time $\sqrt{t}$ and has the form:

$$D = \pi \left(\frac{kh}{4M_m} \right)^2 \qquad [3]$$

where, k is the initial slope of a plot of W_t versus $t^{1/2}$, M_m is the maximum weight gain and h is the thickness of the composite [33,34].

2.4 Mode II interlaminar fracture toughness testing

The Mode II Interlaminar fracture toughness tests were conducted on a Zwick/Roell Z250 universal testing machine to determine the critical strain energy release rate (G_{IIC}) under in-plane shear deformation using three-point-end-notched flexure (3ENF) test based on the ESIS protocol [35], which has not been made yet as an accepted international standard

[36]. Specimens for 3ENF tests, of 25 mm in width (b), 5-6 mm in thickness (2h) and 130 mm in length (L). The delamination length of 55 mm from the start edge until the crack tip using a Teflon film and the spans were 80 mm. The loading was carried out at a constant crosshead displacement rate of 2 mm/min. For each composite laminate, five specimens were tested and the average values were used to determine the fracture energy for initiation and propagation.

In Mode II, the advantages of using ENF test include simplicity and general acceptance. However, the measurements of data reduction in Mode II interlaminar fracture toughness is a complex method and still not fully understood. These are due to the practical reasons such as friction effects, unstable crack propagation and difficult in determining a starter defect [37]. Based on these difficulties in the ENF specimen, the non-linearity (NL) method was used to define the exact point of the crack initiation by employing load-displacement curves. The parameters required for the energy G_C, not only depend on the measurements of load and displacement, but also on the crack length [38]. Therefore, two data reduction methods were used to determine the strain energy release rate, G_{IIC}, and the R-curve. The calculation of load-point compliance was performed , using the equation of $G_{IIC,}$ based on classical simple beam theory (SBT) [39,40].

$$C = \frac{\delta}{P} \quad [4]$$

$$C = \frac{2l^3+3a^3}{8E_1bh^3} \quad [5]$$

The compliance equation is given by

$$G = \frac{P^2}{2b}\frac{dC}{da} \quad [6]$$

The interlaminar fracture toughness can be obtained from [4 to 6]:

$$G_{IIc} = \frac{9P\delta\ \mathrm{a}^2}{2b(3a^3+2L^3)} \quad [7]$$

Where P is load for crack propagation; δ is loading point displacement; a is a crack length measured from the outer pin; L is a half span of 3ENF specimen and b is a beam width.

However, in order to determine the R-curve of delamination growth, the change in compliance with the crack length has been used in the Corrected Calibration Method (CCM) which relies on the least square regression as follows:

$$CN_1 = A + ma^3 \quad [8]$$

Where, N_1 is a large displacement correction factor, A and m are data fitting constants. Hence, G_{IIc}, becomes

$$G_{IIc} = \frac{3mP^2a^2}{2b}\frac{F'}{N_1} \quad [9]$$

Where, F' is an additional large displacements correction factor which was found negligible in 3ENF tests [39,41].

2.5 Scanning electron microscopy (SEM)

The shear-fractured surfaces were examined by SEM JSM 6100 at room temperature. After 3ENF tests, specimens were sputter coated to avoid charging and have a good conductivity with a thin layer of gold/palladium prior to SEM examination. The micrographs of the Mode II fracture mechanism of FVE, FBVEu and FBVEs composite laminates were analysed under dry and wet conditions.

2.6 X-ray computed micro-tomography (µCT)

X-ray computed micro-tomography (µCT) measurements were performed using a Nikon (Xtec) XTH225 to obtain fracture damage characterisation through the thickness of the laminates. µCT methods were used to reconstruct the three-dimensional structure of the samples from a large number of X-ray projection images. VGStudio MAX was used to extract images and the X-ray source powered at 110 kV – 110 uA.

3. Results and discussion

3.1 Sorption behaviour

The weight gain percentage of four different group of samples (FVE, FBVEu, FBVEs and neat VE) vs. square root of time are shown in Fig. 1. Saturation moisture uptake and diffusion coefficient are presented in Table 1. It was found that the maximum percentage of weight gain for FVE, FBVEu, FBVEs and neat VE composite laminates immersed at room temperature for 1008 hours is 5.24, 3.46, 3.41 and 0.78%, respectively. Without basalt hybridisation, flax fibre composites absorbed higher than FBVEu laminates by approximately 34% higher. This is attributed to high cellulose content (71 to 75 %) in the structure of flax fibre that allowed the water molecules to interact with the hydroxyl groups, which led to poor interface between the fibre and matrix [42]. FVE samples absorbed larger amount of water ingress than FBVEu composites. Therefore, the external skin layers of basalt fibre prevented the inner core of flax fibres from the degradation and exhibited a greater resistance to water absorption and it has a superior water repellence behaviour compared to FVE composites. Moreover, water accumulation was reduced in FBVE laminates among their interfacial voids due to improved fibre/matrix interfacial bond [8]. As shown in Fig. 1, there are three-stage mechanisms in different zone for each composite laminates except unreinforced samples with only two stages. At the beginning (stage I), the water absorption rate is rapidly increased with linearity for 15 hours$^{1/2}$ (10 days) in both composites of FVE and FBVE, following a Fickian behaviour at room temperature. After that in (stage II), the curve gradually increased for long time 30 hours$^{1/2}$ (39 days) until saturation reaches a steady state in (stage 3). Water diffusion into polymer composites in phase II involves further displacement of fluid molecules from a region of high concentration to lower concentration. This diffusion is exacerbated through; poor wetting of the fibre, incomplete sizing or grafting, as well as mechanical fatigue. For unreinforced samples, the water uptake process of neat VE composites is linear and slowly increased for just 14 hours$^{1/2}$ (9 days) in (stage I), then quickly reached a stable state because of hydrophobic matrices and do not include any hydrophilic fibres in (stage II). These results of sorption behaviour are an agreement with other results, as reported [8,21].

The diffusion properties of composites were calculated by Fick's law in terms of weight gain percentages of dry specimen immersed in water and the initial slope of the weight gain curve versus square root of time in hours [15]. The diffusion coefficient values for FVE, FBVEu, FBVEs and neat VE composite laminates are presented in Table 1. It can be observed that the moisture uptake and the diffusion coefficient decreased for FBVEu compared to FVE samples without hybridisation by approximately 34% and 29%, respectively. This is ascribed to the hybridisation of hydrophobic basalt layers that preserved the cellulose core layers of composite laminates from degradation during ageing environmental exposure [8]. The water diffusion in thermosetting polymers was found to cause composite laminates swelling and micro cracking, supported by brittle thermosetting resin used. Thus, water penetrated through micro cracks into the interface of the composites consequently caused composite failure [14]. For neat VE composite laminates, when saturation moisture uptake decreased, the diffusion coefficient increased. Similar behaviour has been reported for unsaturated polyester (neat UP) composites [15]. The moisture uptake and the diffusion coefficient were decreased for neat VE when compared to neat UP by approximately 12% and 15%, respectively. It was observed that neat VE composites saturated rapidly than neat UP, This has been reported that the water absorption behaviour was not only depend on the fibre, but also on the type of resin used. This could be caused from the void content and the molecular structure of the resin [43].

3.2 Effect of moisture absorption on Mode II interlaminar fracture toughness

The average load and displacement curves of FVE, FBVEu, FBVEs and neat VE composite laminates were obtained from the 3ENF tests. The curves for both dry and wet specimens are shown in Fig. 2. It can be seen from the figure that the load increased linearly with increase in displacement during the initial stage of loading. These curves show elastic behaviour during deformation, with exception of neat VE samples. For FVE dry composites, the load and displacement increased linearly and then reached to its maximum values of 812 N and 5.2 mm, respectively. However, in the case of FVE wet samples, the displacement continued to increase up to 7.4 mm with decrease in the load by 100 N compared to dry samples. The first reason for this variation is due to the phenomena of plasticisation that could increase the deformation until the fracture point. Secondly, the weak fibre/matrix interface due to water ingress in the interface region. In the case of hybridised composites of FBVEu, both water immersed and dry samples exhibited a sudden drop in load after a maximum load of 696 N and 588 N, respectively. This indicates that the strain energy release rate has already reached the fracture toughness of the material for crack propagation. When the displacement reached 4.5 mm, then the compliance of the dry curve gradually declined, which could initiate matrix cracking in the delamination of composite laminates. It is evidenced that FVE wet samples absorbed higher energy before fracture than FVE dry composites. However, with basalt hybridisation of FBVEu wet specimen absorbed lower energy than FBVEu dry composites. This behaviour is related to the external layers of basalt fibre showing greater resistance to water penetration into fibre/matrix interface due to excellent water repellence behaviour [8]. It is observed that the crack propagation was stable for all samples including stitched composites, but stick-slip crack occurred by arrest crack after the maximum load of FBVEs for both dry and wet samples. The results showed that all composites exhibited ductile fracture except neat VE which showed brittle fracture without any evidence of plastic yielding prior to fracture. Unreinforced vinyl ester showed ostensibly linear behaviour to the point of fracture because of its brittle nature and has low energy absorption before breaking into two pieces. Load and displacement values of saturated samples of neat VE were increased more than that of unsaturated laminates.

3.2.1 Delamination crack growth resistance curve

The experimental results of resistance curves (R-curve) show the relationship between the Mode II strain energy release rate (G_{IIC}) and the delamination length (a). These were obtained to determine the initiation and propagation of a crack length in both conditions; dry and wet. Referring to the published literature on Mode II (3ENF) tests (47, 48), two data reduction methods of CCM and SBT were used to determine the interlaminar fracture toughness. The crack growth results of resistance curves from this study are presented in Fig. 3 for samples of a) FVE, b) FBVEu and c) FBVEs composite laminates. In general, the fracture energy G_{IIC} increased gradually with an increasing delamination growth in all composite laminates and the crack zone was measured between 30 mm and 40 mm. It can be observed that the values obtained from CCM and SBT methods are close to each other and exhibited similar behaviour for both dry and wet composites. However, SBT method had lower values in the fracture energy than CCM of dry composites, whereas in wet samples, the latter showed lower G_{IIC} values than SBT method. This could be related to a large displacement occurred in water-aged samples. As shown in Fig. 3 (a), the average of R-curve obtained for FVE composites, which shows an increasing trend up to a crack growth of 38 mm and 39 mm for dry and wet composites, respectively. With basalt hybridised composites in Fig. 3 (b), the crack length increased from 38 mm to 40 mm compared to FVE dry composites showing that high resistance to delamination due to the external of basalt layers, which contributed to increasing crack propagation resistance. It was observed that the crack length reduced for FBVEu wet laminates from 40 mm to 39 mm compared to FBVEu dry ones. This behaviour could be attributed to the reduction in fibre/matrix interfacial strength due to the moisture absorption that resulting a reduction to crack propagation; this however improved the resistance to crack initiation because of increasing in matrix ductility [45]. The results for stitched composites of FBVEs are shown in Fig. 3 (c), it can be seen that the lowest crack length for stitched composites with only increased by 5-6 mm due to the arrest to crack propagation of stitching yarn, while unstitched composites of FBVEu growth up to 9-10 mm.

3.2.2 Fracture energy

The results from Mode II strain energy release rates of $G_{IIC\ init.}$ and $G_{IIC\ prop.}$ are shown in Fig. 4, depicting FVE, FBVEu, FBVEs and neat VE composite laminates at dry and wet conditions. It can be noted that the initiation and propagation of fracture energy increased with increasing the moisture content of FVE wet composites as shown in Fig. 4 (a). There are some reasons for increase in the strain energy release rate G_{IIC} after water absorption; firstly water molecules is a key factor for a plasticiser that influenced the fibres and matrix by distributing the mechanical integrity of composite laminates [46], and secondly, flax fibres are susceptible to absorb high amount of water due to its hydrophilic nature and consist of high cellulose which would effect on the structure and dimension of the fibres [47]. Similar observations have been reported on the effect of water absorption on the mechanical properties of hemp fibre reinforced unsaturated composites for both flexural and tensile strains [15]. With basalt hybridisation in Fig. 4 (b), the resistance to crack initiation of saturation samples were improved due to matrix ductility; however, this was declined by a reduction in the interfacial strength of fibre-matrix and causing a decreased in the resistance to crack propagation of FBVEu wet composites. It is clear that in Fig. 4 (c), the interlaminar fracture toughness of crack growth was reduced significantly due to stitching. This could be ascribed to fibres damage caused by thread when needle punched into the composite laminates during the process of stitching [21]. This could also have created a stress concentration region. Therefore, stitched woven composites led to reduce the interlaminar fracture toughness of $G_{IIC\ prop.}$, caused damage to the structural performance under shear fracture and reduces its delamination resistance. This behaviour under stitched samples is in close agreement with our previous experimental results on Mode I interlaminar fracture toughness [21] and also other recently published works on the mechanical properties of low velocity impact test [32]. After water immersion in Fig. 4 (d), neat VE composites were found the fracture energy is higher than neat VE dry composites.

The average values of the interlaminar fracture toughness of $G_{IIC\ init.}$ and $G_{IIC\ prop.}$ for dry and wet composite specimens using CCM and SBT methods are summarised in in Fig. 4. It was found that hybrid composites of FBVEu improved the interlaminar fracture toughness of the initiation and propagation when compared to FVE dry samples by approximately 58% and 21%, respectively. Consequently, hybridisation with basalt fibres placed in the outer layers improved the Mode II interlaminar fracture toughness of natural fibres reinforced composite laminates as well as superior ageing resistance. Saturation results of $G_{IIC\ init.}$ and $G_{IIC\ prop.}$ for FVE wet composites were increased by 29% and 33%, respectively compared to FVE dry specimens, due to high moisture absorption from the hydrophilic nature of natural fibres; particularly flax fibres which consist of high cellulose about 71-75% [42] and the plasticisation of the matrix [48]. In addition, the presence of moisture increased the resistance to crack initiation of FBVEu wet composites. However, it tended to cause a reduction in the propagation of fracture energy. This has resulted to reduction in the interfacial strength between the fibres and matrix due to the presence of the water into the interface. Hence, it increased matrix ductility [45]. In the case of stitched composites, FBVEs samples had the highest resistance to crack initiation of fracture toughness for both dry and wet composites than unstitched composites. It was observed that stitching of natural fibre composites through-thickness reinforcement can enhanced the interlaminar fracture toughness [49]. However, it was also observed that stitching led to a notable reduction in the in-plane mechanical properties and the delamination resistance to crack propagation [21,32,49]. In this study, the interlaminar fracture toughness, $G_{IIC\ prop.}$ of stitched composites were significantly lower than unstitched composites of FBVEu dry laminates by 36%. The reason is that stitching can create resin-rich pockets at the crack tip zone and cause in-plane fibre damage. As shown in Fig. 5 (a), misalignment of in-plane fibres around the stitch zone is attributed to large reduction in the interlaminar shear strength of FBVEs samples, whereas in Fig. 5 (b), there is a good fibres alignment of unstitched composites of FVE. It has been reported that stitching can lead to disruption of the fibre alignment and misaligned yarns between the weft and warp of woven tows [21,50]. The results in Fig. 4 (d), is an agreement values with other thermosetting results such as polyester [25]; the critical strain energy release rate G_{IIC} of neat polyester and neat VE composites was about 100 J/m^2 and 158 J/m^2, respectively. The fracture energy of $G_{IIC\ init.}$ for example increased for neat VE from 157.84 J/m^2 to 239.85 J/m^2 without hybridisation of FVE composites, while with basalt hybridised of FBVEu specimens increased to 369.54 J/m^2.

3.3 Morphology of shear fracture surfaces

The shear fracture surfaces of the 3ENF specimens after testing were evaluated by SEM analysis at dry and wet conditions. Fig. 6 shows the fracture surfaces of the dry composites after Mode II failure. The shear fracture of deformed fibres is dissipative process which requires more energy and high fracture resistance for FVE composites as shown in Fig. 6 (a). As stated in the literature that flax fibres possess microstructural defects such as kink bands and nodes or dislocations [18,42]. At higher magnification of flax fibres (Fig. 6 (b)), shear kink bands led to stress concertation in the matrix and fibres resulting into poor internal adhesion. Fracture occurred mostly at the interface of fibre/matrix as revealed on the fracture surfaces by the bare fibres as a consequence of poor interfacial bonding [51]. Furthermore, micro cracks inside thermosetting matrix facilitated penetration from the moisture of flax fibres that consist mainly of cellulose and hemicellulose which is related to high moisture absorption [8]. Therefore, this weak fibre/matrix adhesion led to reduction in the interlaminar fracture toughness of FVE composites. It was observed that the capability to absorb fracture energy is higher for the hybrid composites of FBVEu than flax laminates of FVE, regardless of water immersed specimens. This means that using of basalt fibres as an external reinforcing element shows improvement of the Mode II interlaminar fracture toughness of flax laminates. It is evident from microscopic images in Fig. 6 (c) that the presence of basalt fibres increased the resistance to crack propagation despite the increased delamination of FBVEu composites. Hence, lower degradation in the interlaminar fracture toughness properties of FBVEu can be attributed to the properties of basalt fibres when hybridised on the outer layers of the laminates to prevent the internal layers from the degradation. This phenomenon was also reported by Fiore et al. [51] on the flexural and impact properties. For stitched composites, the stitch yarn contributed to an increase of interlaminar fracture toughness of $G_{IIC\ init.}$ than unstitched composites, because of the energy dissipated directly to the front of the crack tip. However, when the crack propagated until the stitch zone, the fracture energy of $G_{IIC\ prop.}$ decreased significantly compared to unstitched samples. Thus, matrix cracking occurred in the vicinity of stitch yarn which could create resin pockets and then deteriorate the in-plane properties, as seen in Fig. 6 (d). These microscopic results commonly occurs on Mode II (3ENF) tests [52].

SEM micrographs of shear fracture surfaces for water-immersed samples are shown in Fig. 7. There are some differences between the images of dry and wet samples because of the degradation affected by the presence of water molecules. It shows that the fracture surfaces of water-immersed samples were more exposed than dry composites, especially those samples without hybridisation. In Fig. 7 (a), voids and cracks on the surface of FVE composites caused penetration damage into the laminates due to the hydrophilic nature of flax fibres. This is an indication of the reduction in the fibre/matrix interfacial strength due to hydrolysis. Basalt hybridisation of FBVEu laminates improved the interlaminar fracture toughness and the water repellence properties. It can be seen that from Fig. 7. (b), matrix degradation mostly occurred in the matrix interface rather than fibres with no any evidence of voids and cavity on the shear fracture surfaces of FBVEu and FBVEs wet composites. The fractured surface of stitched composites are shown in Fig. 7 (c). Extensive fibre bundle fracture and fibre bridging can be clearly observed at higher magnification in Fig. 7 (d). This finding is in agreement with our previous results on Mode I [21].

4. Conclusions

The present study investigated the effects of water absorption on the interlaminar fracture toughness behaviour of woven flax and flax/basalt reinforced vinyl ester composite laminates. The Mode II experimental works were performed under 3ENF tests. Evaluation of the fracture energy initiation and propagation as well as the crack length under dry and wet conditions using CCM and SBT methods were carried out.

The results showed that basalt fibre hybridised composites improved the interlaminar fracture toughness for initiation and propagation when compared to FVE dry specimens. Furthermore, the crack length of FBVEu dry composites exhibited high resistance to delamination due to the external of basalt fibre layers and showed an increased crack propagation resistance. It was noted that in stitched composites of FBVEs, stitches yarn effectively arrested the delamination and contributed to increase the fracture energy of $G_{IIC\ init.}$ by 62% but the interlaminar fracture toughness of $G_{IIC\ prop.}$ decreased by 36%. The fracture energy of $G_{IIC\ init.}$ for neat VE increased from 157.84 J/m^2 to 239.85 J/m^2 with reinforcement of flax fibre composites. The SBT method showed lower values in the fracture energy than CCM method at dry conditions. It was observed that flax fibre composites without basalt hybridisation absorbed higher moisture uptake than FBVEu laminates with percentage of 34%, and FVE wet samples absorbed higher energy before fracture than FVE dry composites. However, with basalt hybridisation of FBVEu wet specimen absorbed lower energy than FBVEu dry composites. This is attributed to the external skin layers of basalt fibres, which exhibited a greater resistance to water absorption and prevented the inner core of flax fibres from the degradation.

References

[1] D.B. Dittenber, H.V.S. Gangarao, Critical review of recent publications on use of natural composites in infrastructure, Compos. Part A Appl. Sci. Manuf. 43 (2012) 1419–1429.

[2] V.K. Thakur, M.K. Thakur, Processing and characterization of natural cellulose fibers/thermoset polymer composites, Carbohydr. Polym. 109 (2014) 102–117.

[3] N. Venkateshwaran, A. ElayaPerumal, A. Alavudeen, M. Thiruchitrambalam, Mechanical and water absorption behaviour of banana/sisal reinforced hybrid composites, Mater. Des. 32 (2011) 4017–4021.

[4] A.K. Bledzki, J. Gassan, Composites reinforced with cellulose based fibres, Prog. Polym. Sci. 24 (1999) 221–274.

[5] H.N. Dhakal, Z.Y. Zhang, N. Bennett, A. Lopez-Arraiza, F.J. Vallejo, Effects of water immersion ageing on the mechanical properties of flax and jute fibre biocomposites evaluated by nanoindentation and flexural testing, J. Compos. Mater. 48 (2014) 1399–1406.

[6] C.P.L. Chow, X.S. Xing, R.K.Y. Li, Moisture absorption studies of sisal fibre reinforced polypropylene composites, Compos. Sci. Technol. 67 (2007) 306–313.

[7] O. Faruk, A.K. Bledzki, H.-P. Fink, M. Sain, Biocomposites reinforced with natural fibers: 2000–2010, Prog. Polym. Sci. 37 (2012) 1552–1596.

[8] V. Fiore, T. Scalici, L. Calabrese, A. Valenza, E. Proverbio, Effect of external basalt layers on durability behaviour of flax reinforced composites, Compos. Part B Eng. 84 (2016) 258–265.

[9] V. Fiore, T. Scalici, F. Sarasini, J. Tirilló, L. Calabrese, Salt-fog spray aging of jute-basalt reinforced hybrid structures: Flexural and low velocity impact response, Compos. Part B Eng. 116 (2017) 99–112.

[10] H.N. Dhakal, F. Sarasini, C. Santulli, J. Tirillò, Z. Zhang, V. Arumugam, Effect of basalt fibre hybridisation on post-impact mechanical behaviour of hemp fibre reinforced composites, Compos. Part A Appl. Sci. Manuf. 75 (2015) 54–67.

[11] F. Sarasini, J. Tirillò, M. Valente, T. Valente, S. Cioffi, S. Iannace, L. Sorrentino, Effect of basalt fiber hybridization on the impact behavior under low impact velocity of glass/basalt woven fabric/epoxy resin composites, Compos. Part A Appl. Sci. Manuf. 47 (2013) 109–123.

[12] V. Fiore, T. Scalici, D. Badagliacco, D. Enea, G. Alaimo, A. Valenza, Aging resistance of bio-epoxy jute-basalt hybrid composites as novel multilayer structures for cladding, Compos. Struct. 160 (2016) 1319–1328.

[13] J. Sim, C. Park, D.Y. Moon, Characteristics of basalt fiber as a strengthening material for concrete structures, Compos. Part B Eng. 36 (2005) 504–512.

[14] L.A. Pothan, S. Thomas, Effect of hybridization and chemical modification on the water-absorption behavior of banana fiber–reinforced polyester composites, J. Appl. Polym. Sci. 91 (2004) 3856–3865.

[15] H.N. Dhakal, Z.Y. Zhang, M.O.W. Richardson, Effect of water absorption on the mechanical properties of hemp fibre reinforced unsaturated polyester composites, Compos. Sci. Technol. 67 (2007) 1674–1683.

[16] Y. Li, Y.-W. Mai, L. Ye, Effects of fibre surface treatment on fracture-mechanical properties of sisal-fibre composites, Compos. Interfaces. 12 (2005) 141–163.

[17] Q. Liu, M. Hughes, The fracture behaviour and toughness of woven flax fibre reinforced epoxy composites, Compos. Part A Appl. Sci. Manuf. 39 (2008) 1644–1652.

[18] M. Hughes, J. Carpenter, C. Hill, Deformation and fracture behaviour of flax fibre reinforced thermosetting polymer matrix composites, J. Mater. Sci. 42 (2007) 2499–2511.

[19] K.J. Wong, S. Zahi, K.O. Low, C.C. Lim, Fracture characterisation of short bamboo fibre reinforced polyester composites, Mater. Des. 31 (2010) 4147–4154.

[20] N. Ranganathan, K. Oksman, S.K. Nayak, M. Sain, Structure property relation of hybrid biocomposites based on jute , viscose and polypropylene : The effect of the fibre content and the length on the fracture toughness and the fatigue properties,

Compos. Part A Appl. Sci. Manuf. 83 (2016) 169–175.

[21] F.A. Almansour, H.N. Dhakal, Z.Y. Zhang, Effect of water absorption on Mode I interlaminar fracture toughness of flax / basalt reinforced vinyl ester hybrid composites, Compos. Struct. 168 (2017) 813–825.

[22] H. Hajiha, M. Sain, Model development for work of fracture of hybrid composites, J. Appl. Polym. Sci. (2017).

[23] S. Keck, M. Fulland, Effect of fibre volume fraction and fibre direction on crack paths in flax fibre-reinforced composites, Eng. Fract. Mech. (2016).

[24] S. Wong, R. a. Shanks, A. Hodzic, Mechanical behavior and fracture toughness of poly(L-lactic acid)-natural fiber composites modified with hyperbranched polymers, Macromol. Mater. Eng. 289 (2004) 447–456.

[25] M. Hughes, C.A.S. Hill, J.R.B. Hague, The fracture toughness of bast fibre reinforced polyester composites. Part 1 Evaluation and analysis, J. Mater. Sci. 7 (2002) 4669–4676.

[26] F.A. Almansour, H.N. Dhakal, Z.Y. Zhang, H. Ghasemnejad, Effect of hybridization on the mode II fracture toughness properties of flax/vinyl ester composites, Polym. Compos. (2015).

[27] X.K. Zhu, J.A. Joyce, Review of fracture toughness (G, K, J, CTOD, CTOA) testing and standardization, Eng. Fract. Mech. 85 (2012) 1–46.

[28] M.V. Hosur, U.K. Vaidya, C. Ulven, S. Jeelani, Performance of stitched/unstitched woven carbon/epoxy composites under high velocity impact loading, Compos. Struct. 64 (2004) 455–466.

[29] K. Dransfield, C. Baillie, Y. Mai, Improving the delamination resistance of CFRP by stitching. A Review, Compos. Sci. Technol. 50 (1994) 305–317.

[30] B. V Sankar, S.K. Sharmab, Mode II delamination toughness of stitched graphite/epoxy textile composites, Compos. Sci. Technol. 57 (1997) 729–737.

[31] L.K. Jain, K.A. Dransfieldb, Y. Ma, On the effects of stitching in CFRPs-II. Mode II delamination toughness, Compos. Sci. Technol. 58 (1998) 829–837.

[32] M. Ravandi, W.S. Teo, L.Q.N. Tran, M.S. Yong, T.E. Tay, Low velocity impact performance of stitched flax / epoxy composite laminates, Compos. Part B. 117 (2017) 89–100.

[33] J. Crank, the Mathematics of Diffusion, 1975.

[34] A. Espert, F. Vilaplana, S. Karlsson, Comparison of water absorption in natural cellulosic fibres from wood and one-year crops in polypropylene composites and its

influence on their mechanical properties, Compos. Part A Appl. Sci. Manuf. 35 (2004) 1267–1276.

[35] Davies P, Protocols for interlaminar fracture testing of composites, (1993).

[36] a. J. Brunner, B.R.K. Blackman, P. Davies, A status report on delamination resistance testing of polymer–matrix composites, Eng. Fract. Mech. 75 (2008) 2779–2794.

[37] P. Davies, B. Blackman, A. Brunner, Standard test methods for delamination resistance of composite materials: current status, Appl. Compos. Mater. 5 (1998) 345–364. doi:10.1023/a:1008869811626.

[38] T.K. O'Brien, Interlaminar fracture toughness: the long and winding road to standardization, Compos. Part B Eng. 29 (1998) 57–62.

[39] H. Hadavinia, H. Ghasemnejad, Effects of Mode-I and Mode-II interlaminar fracture toughness on the energy absorption of CFRP twill/weave composite box sections, Compos. Struct. 89 (2009) 303–314.

[40] K.N. Russell, A.J. and Street, Factors Affecting the Interlaminar Fracture Energy of Graphite/Epoxy Laminates, in: K.K.& S.U. ed. T. Hayashi (Ed.), Prog. Sci. Eng. Compos., ICCM-IV, Tokyo, 1982: p. 279.

[41] A.P. D.R. Moore, J.G. Williams, Fracture Mechanics Testing Methods for Polymers, Adhesives and Composites, Elsevier, Oxford, 2001.

[42] L. Yan, N. Chouw, K. Jayaraman, Flax fibre and its composites – A review, Compos. Part B Eng. 56 (2014) 296–317.

[43] H.J. Kim, D.W. Seo, Effect of water absorption fatigue on mechanical properties of sisal textile-reinforced composites, Int. J. Fatigue. 28 (2006) 1307–1314.

[44] R. Zenasni, B. a. Saadi, Moisture Effect on the Interlaminar Resistance of Woven Fabric Thermoplastic Composite, J. Thermoplast. Compos. Mater. 19 (2006) 715–729.

[45] N.H. Nash, T.M. Young, W.F. Stanley, The influence of a thermoplastic toughening interlayer and hydrothermal conditioning on the Mode-II interlaminar fracture toughness of Carbon/Benzoxazine composites, Compos. Part A Appl. Sci. Manuf. 81 (2016) 111–120.

[46] G. Huang, H. Sun, Effect of water absorption on the mechanical properties of glass/polyester composites, Mater. Des. 28 (2007) 1647–1650.

[47] J. Biagiotti, D. Puglia, J.M. Kenny, A Review on Natural Fibre- Based Composites-Part I, J. Nat. Fibers. 1 (2008) 37–41.

[48] N.H. Nash, T.M. Young, W.F. Stanley, The reversibility of Mode-I and -II interlaminar fracture toughness after hydrothermal aging of Carbon/Benzoxazine

composites with a thermoplastic toughening interlayer, Compos. Struct. 152 (2016) 558–567.

[49] M. Ravandi, W.S. Teo, L.Q.N. Tran, M.S. Yong, T.E. Tay, The effects of through-the-thickness stitching on the Mode I interlaminar fracture toughness of flax/epoxy composite laminates, Mater. Des. 109 (2016) 659–669.

[50] A.P. Mouritz, B.N. Cox, A mechanistic interpretation of the comparative in-plane mechanical properties of 3D woven, stitched and pinned composites, Compos. Part A Appl. Sci. Manuf. 41 (2010) 709–728.

[51] P. Suppakul, S. Bandyopadhyay, The effect of weave pattern on the mode-I interlaminar fracture energy of E-glass/vinyl ester composites, Compos. Sci. Technol. 62 (2002) 709–717.

[52] P. Compston, P.-Y. Jar, P.J. Burchill, K. Takahashi, The effect of matrix toughness and loading rate on the mode-II interlaminar fracture toughness of glass-fibre/vinyl-ester composites, Compos. Sci. Technol. 61 (2001) 321–333.

Table 1 Moisture uptake and diffusion coefficient of FVE, FBVEu, FBVES and neat VE composite laminates immersed in distilled water at room temperature.

Type of Sample	Saturation moisture uptake M_m (%)	Initial slope of plot (*k*) *M(t)* versus $t^{1/2}$	Diffusion Coefficient, D, x10-3(m^2/s)
FVE	5.24	0.25	1.50776E-06
FBVEu	3.46	0.15	1.0739E-06
FBVEs	3.41	0.15	1.04705E-06
neat VE	0.78	0.07	4.65357E-06
neat UPE*	0.87	0.10	5.714E-06

*for comparison purpose

Fig. 1. Weight gain as a function of time for 3ENF specimens of FVE, FBVEu, $FBVE_S$ and neat VE composite laminates exposed to distilled water at room temperature.

Fig. 2. Load versus displacement curves for Mode II dry and wet samples.

Fig. 3. Resistance curves (R-curve) of Mode II (3ENF) tests for both dry and wet samples of (a) FVE, (b) FBVEu and (c) FBVEs composite specimens using CCM and SBT methods.

Fig. 4. Mode II strain energy release rate, G_{IIC} for initiation and propagation toughness obtained from 3ENF tests at dry and wet conditions of (a) FVE, (b) FBVEu, (c) FBVEs and (d) neat VE composite specimens using CCM and SBT methods.

Fig. 5. Computed micro-tomography (µCT) images of the reconstructed 2D slice in x-z plane from backside for (a) FBVEs and (b) FVE composites.

Fig. 6. SEM images of Mode II fracture surfaces at dry specimens of (a) shear fracture which deformed fibres for FVE. (b) shear kink bands or nodes lead to failure of flax fibres. (c) fibre delamination and breakage of FBVEu. (d) matrix cracking caused by stitching for FBVEs.

Fig. 7. SEM images of Mode II fracture surfaces at wet specimens of (a) shear fractured fibres and voids due to moisture for FVE. (b) matrix degrdation of FBVEu. (c) fractured stitch fibres of FBVEs. (d) Extensive fibre bundle breakage and bridging of FBVEs.

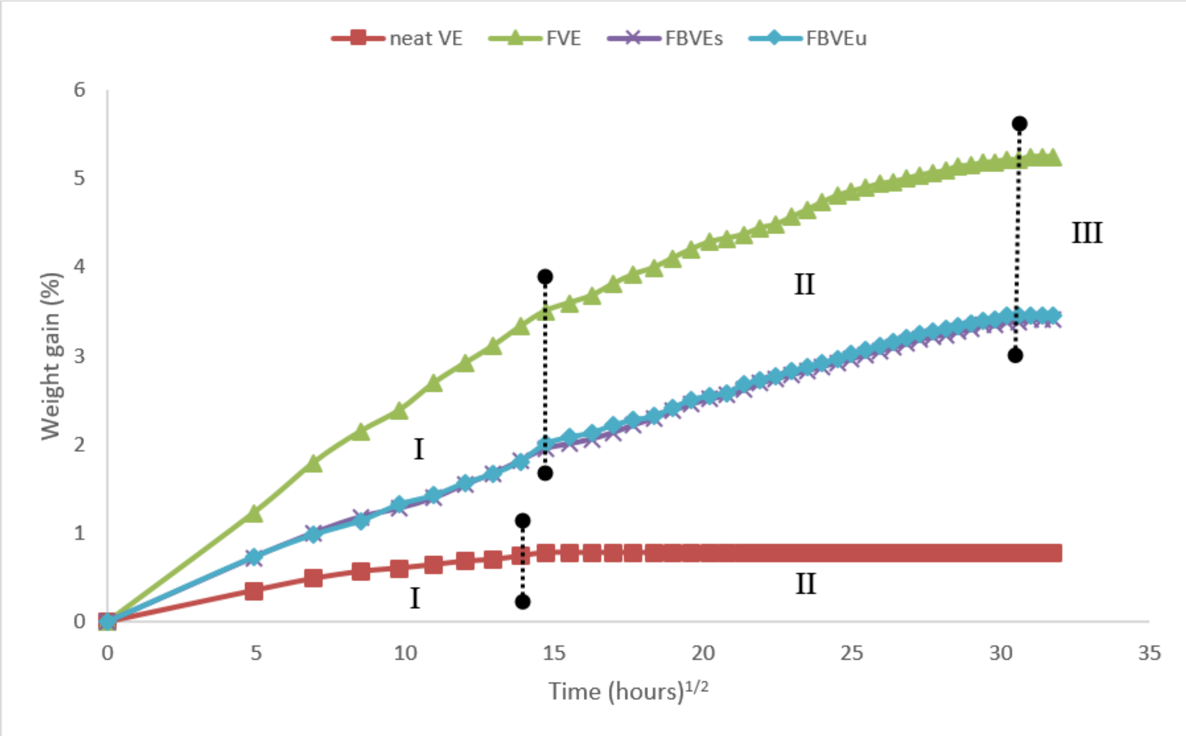

Fig. 1. Weight gain as a function of time for 3ENF specimens of FVE, FBVEu, $FBVE_S$ and neat VE composite laminates exposed to distilled water at room temperature.

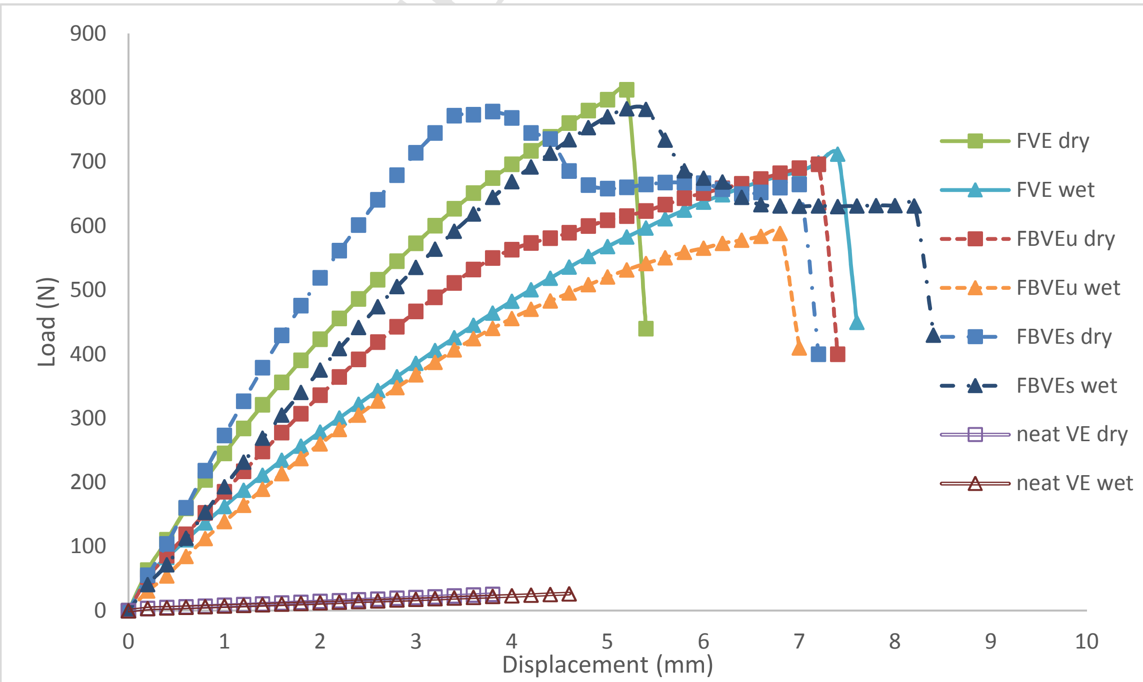

Fig. 2. Load versus displacement curves for Mode II dry and wet samples.

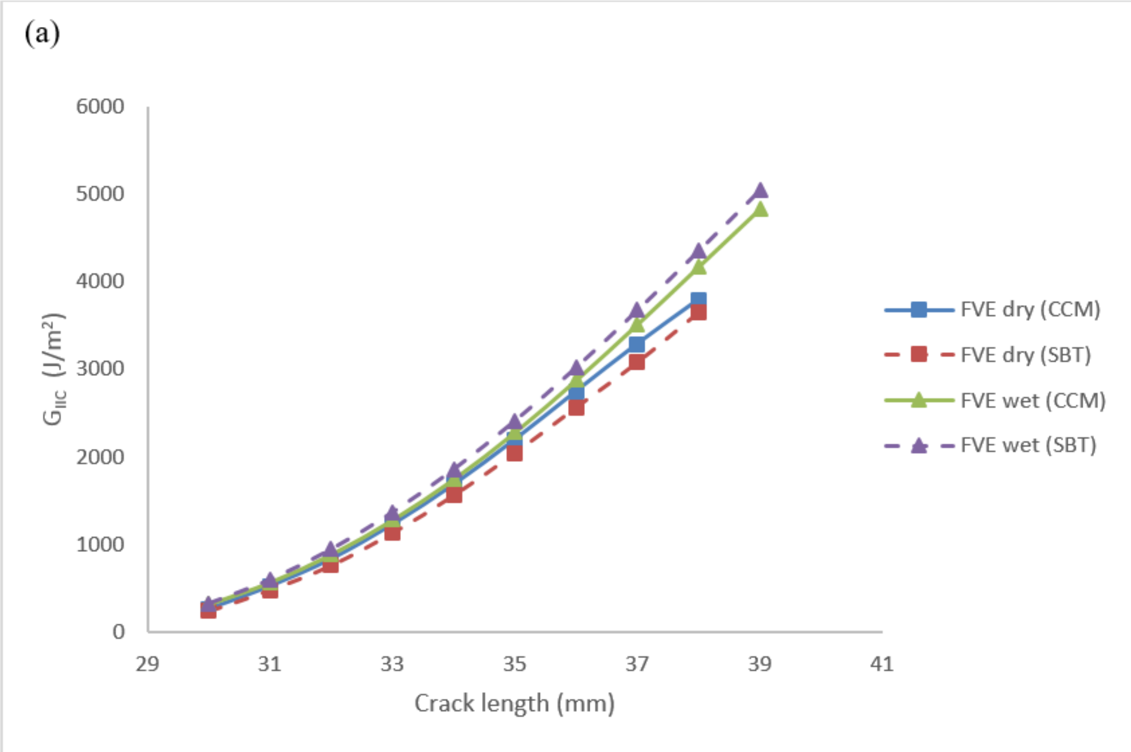
(a)
6000
5000
4000
3000
2000
1000
0
G_{IIC} (J/m^2)
29
31
33
35
37
39
41
Crack length (mm)
FVE dry (CCM)
FVE dry (SBT)
FVE wet (CCM)
FVE wet (SBT)

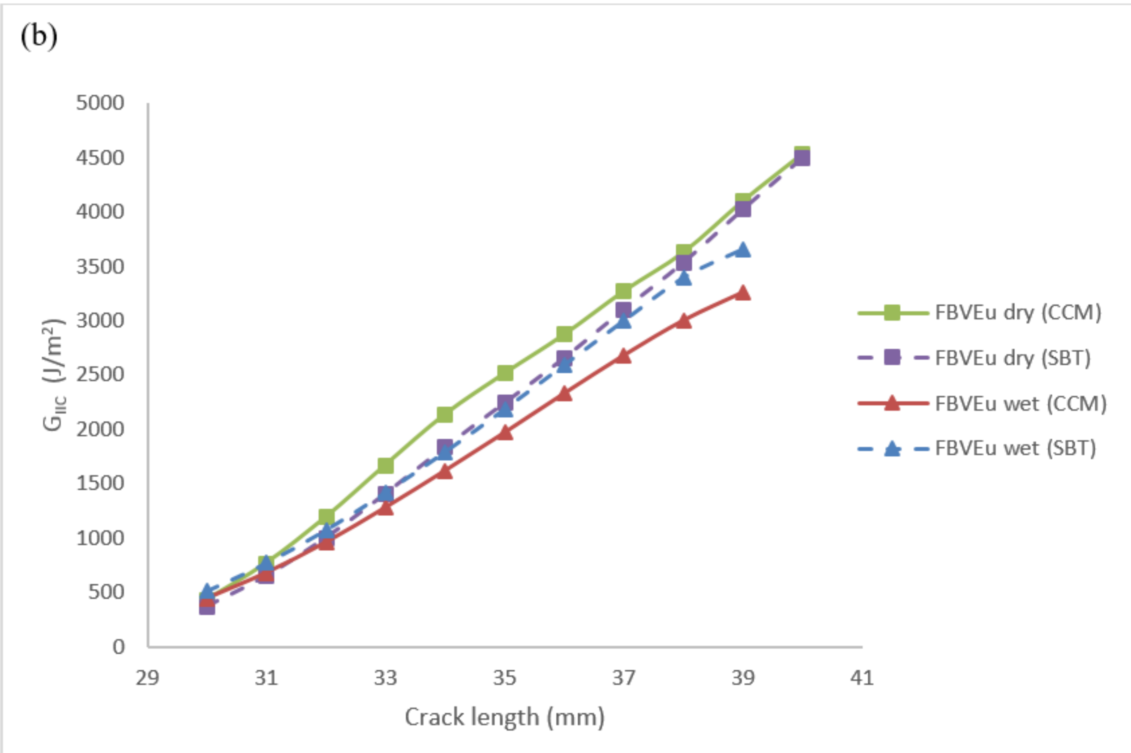
(b)
5000
4500
4000
3500
3000
2500
2000
1500
1000
500
0
G_{IIC} (J/m^2)
29
31
33
35
37
39
41
Crack length (mm)
FBVEu dry (CCM)
FBVEu dry (SBT)
FBVEu wet (CCM)
FBVEu wet (SBT)

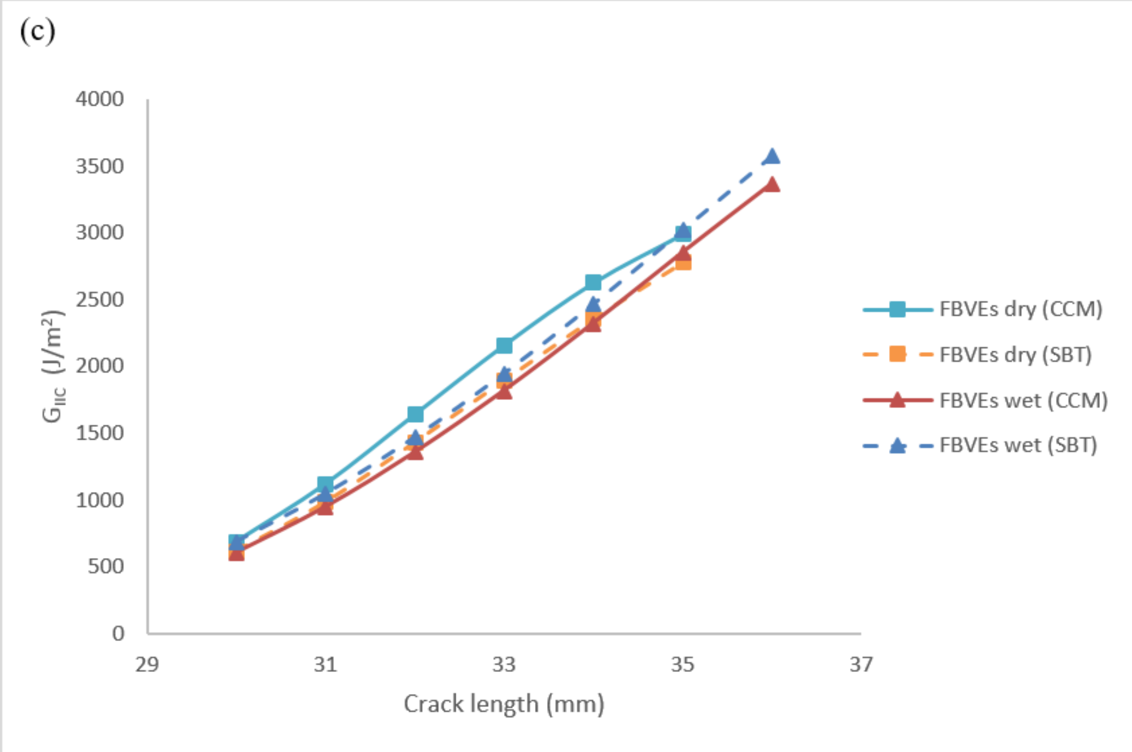

Fig. 3. Resistance curves (R-curve) of Mode II (3ENF) tests for both dry and wet samples of (a) FVE, (b) FBVEu and (c) FBVEs composite specimens using CCM and SBT methods.

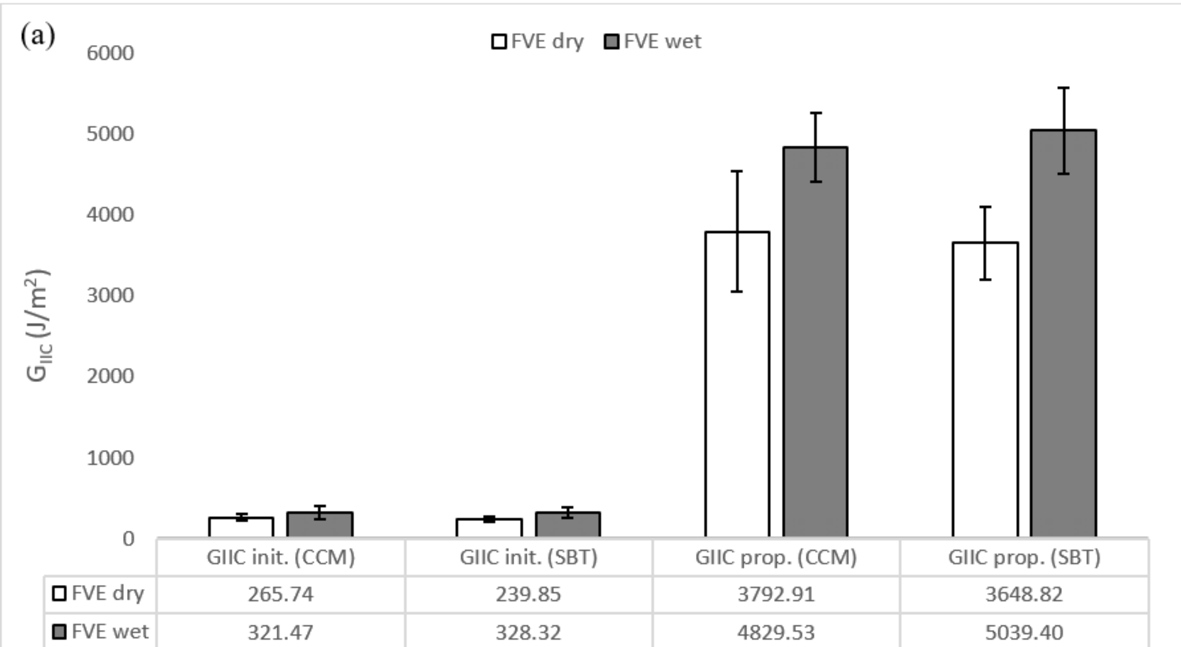

	GIIC init. (CCM)	GIIC init. (SBT)	GIIC prop. (CCM)	GIIC prop. (SBT)
FVE dry	265.74	239.85	3792.91	3648.82
FVE wet	321.47	328.32	4829.53	5039.40

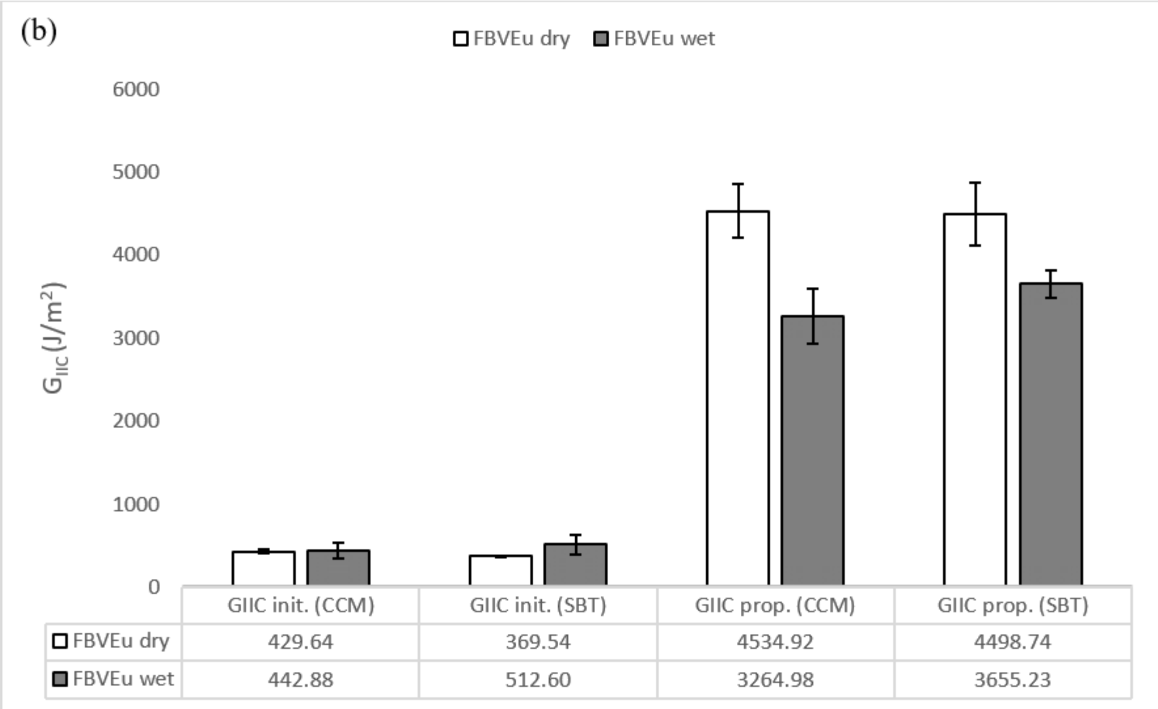
(b)
FBVEu dry
FBVEu wet
6000
5000
4000
3000
2000
1000
0
G_{IIC} (J/m^2)
GIIC init. (CCM)
GIIC init. (SBT)
GIIC prop. (CCM)
GIIC prop. (SBT)
FBVEu dry 429.64 369.54 4534.92 4498.74
FBVEu wet 442.88 512.60 3264.98 3655.23

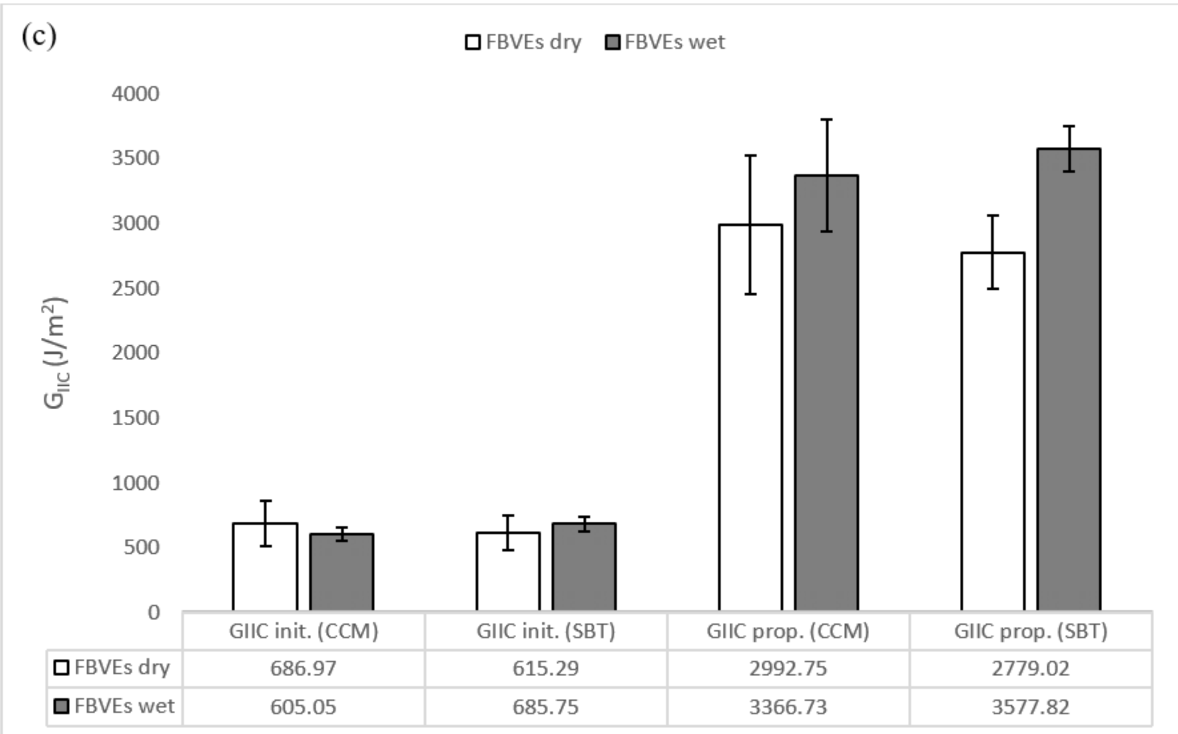
(c)
FBVEs dry
FBVEs wet
4000
3500
3000
2500
2000
1500
1000
500
0
G_{IIC} (J/m^2)
GIIC init. (CCM)
GIIC init. (SBT)
GIIC prop. (CCM)
GIIC prop. (SBT)
FBVEs dry 686.97 615.29 2992.75 2779.02
FBVEs wet 605.05 685.75 3366.73 3577.82

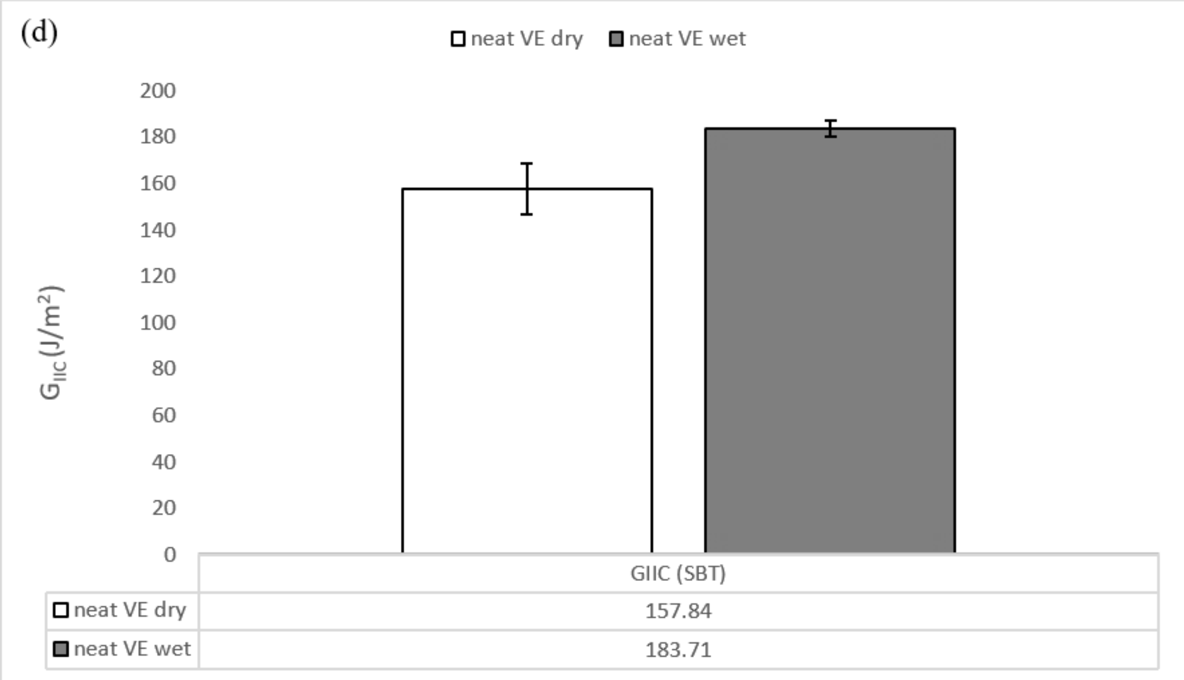

Fig. 4. Mode II strain energy release rate, G_{IIC} for initiation and propagation toughness obtained from 3ENF tests at dry and wet conditions of (a) FVE, (b) FBVEu, (c) FBVEs and (d) neat VE composite specimens using CCM and SBT methods.

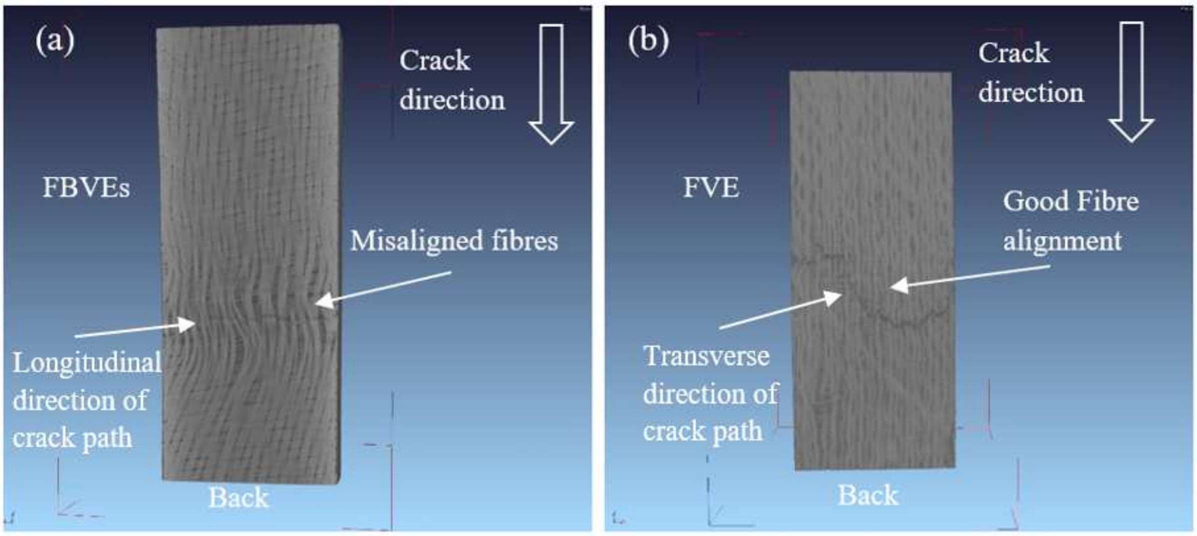

Fig. 5. Computed micro-tomography (µCT) images of the reconstructed 2D slice in x-z plane from backside for (a) FBVEs and (b) FVE composites.

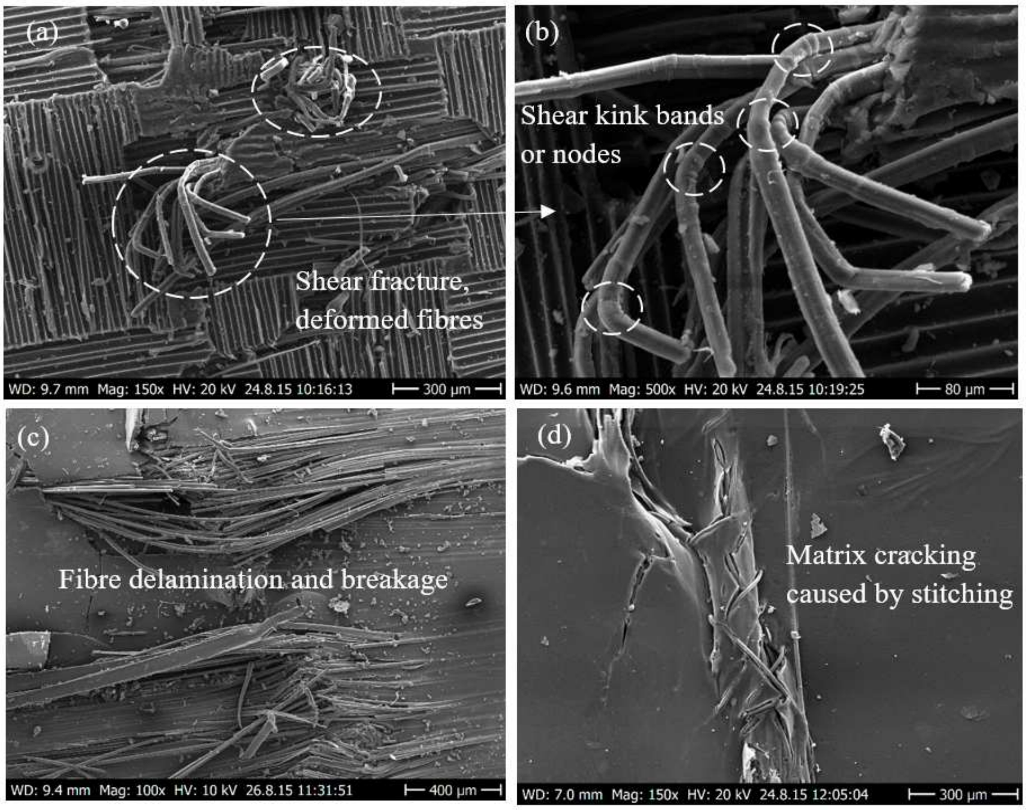

Fig. 6. SEM images of Mode II fracture surfaces at dry specimens of (a) shear fracture which deformed fibres for FVE. (b) shear kink bands or nodes lead to failure of flax fibres. (c) fibre delamination and breakage of FBVEu. (d) matrix cracking caused by stitching for FBVEs.

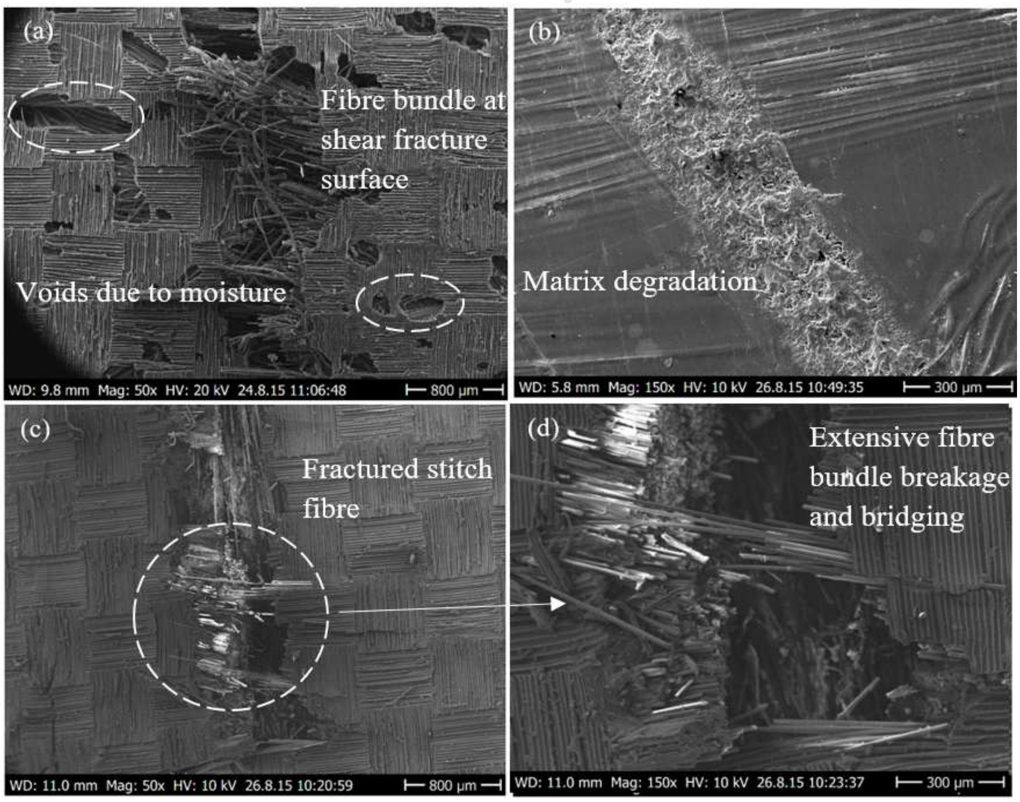

Fig. 7. SEM images of Mode II fracture surfaces at wet specimens of (a) shear fractured fibres and voids due to moisture for FVE. (b) matrix degrdation of FBVEu. (c) fractured stitch fibres of FBVEs. (d) Extensive fibre bundle breakage and bridging of FBVEs.